

Quantum-enhanced Markov Chain Monte Carlo for systems larger than your Quantum Computer

Stuart Ferguson^{1, a}, Petros Wallden^{2, a}

^a*Quantum Software Lab, School of Informatics, The University of Edinburgh, Edinburgh, United Kingdom*

Abstract

Quantum computers theoretically promise computational advantage in many tasks, but it is much less clear how such advantage can be maintained when using existing and near-term hardware that has limitations in the number and quality of its qubits. One promising application was proposed in Layden et al [1] where a method to reduce the thermalisation time required when sampling from hard probability distribution was introduced as a Quantum-enhanced Markov Chain Monte Carlo (QeMCMC) approach. In [1] the size of the required quantum computer scales linearly with the problem, putting limitations on the sizes of systems that one can consider. In this work we introduce a framework to coarse grain the algorithm in such a way that the quantum computation can be performed using, multiple times, smaller quantum computers and we term the method the Coarse Grained Quantum-enhanced Markov Chain Monte Carlo (CGQeMCMC). Example strategies within this framework are put to the test, with the quantum speedup of [1] persisting while using only \sqrt{n} simulated qubits where n is the number of qubits required in the original QeMCMC – a quadratic reduction in resources. The coarse graining framework has the potential to be practically applicable in the near term as it requires very few qubits to approach classically intractable problem instances, here only 6 simulated qubits suffice to gain advantage compared to standard classical approaches when investigating the magnetisation of a 36 spin system. Our method is also adjustable to quantum hardware specifications, and it appears that it can be easily combined with other techniques both classical and quantum.

May 8, 2024

1. Introduction

Sampling from hard distributions is a problem ubiquitous in science, technology, finance and statistics. While there are well understood families of traditional computational methods such as the Markov Chain Monte Carlo (MCMC) [2, 3] that attempt to address this challenge, the advent of quantum computing offers a promising avenue for considerably more efficient solutions in randomised algorithms such as [4] and [5].

Current Quantum Processing Units (QPUs) are labelled as ‘Noisy Intermediate-Scale Quantum’ (NISQ) devices, meaning that although they exhibit remarkable quantum phenomena they have strict limitations in the number of available qubits and the quality of qubits and operations that are very error-prone. In this era where full quantum error-correction is out of reach, one must explore algorithms that are not only robust to noise but also as efficient in the number of qubits as possible. One algorithm that addresses the former requirement is the Quantum-enhanced Markov Chain Monte Carlo (QeMCMC) of [1]. It introduces an elegant way to enhance the classical MCMC by “quantising” one part of the classical MCMC algorithm: namely the proposal step. The method has also been extended, by application to Hamiltonian Monte-Carlo [6] and Variational algorithms [7].

In this paper, we propose a way to significantly reduce the qubit requirement of the QeMCMC, while maintaining quantum speedup over the classical MCMC in the low temperature

limit³. This is done by Coarse Graining (CG) the problem instance – an Ising model lattice – in such a way that each subset “group” of the lattice can be evaluated in separate quantum computations, even on different QPU’s in parallel. In this way, it is predicted that one can use a QPU with as few as $O(\sqrt{n})$ qubits and still achieve quantum advantage. We call this method the Coarse Grained Quantum-enhanced Markov Chain Monte Carlo (CGQeMCMC).

The way in which QeMCMC [1] achieves quantum advantage is by reducing the thermalisation time of a Markov chain. This is the number of steps taken to reach the stationary distribution which you wish to sample from. Here we need to make a distinction between the cost of proving that thermalisation is achieved fast (a task needed to prove the performance of the algorithm) and the use of our CGQeMCMC practically for some task. For the former, the primary method of analysing thermalisation is by spectral gap analysis, a well known and unambiguous figure of merit. Calculating the spectral gap, however, is an entirely different process from MCMC and is exponentially more expensive, restricting our spectral gap analysis to 10 spins. For the latter, we use Markov chains to estimate an example observable – magnetisation – and in this case we consider a system of 36 spins to experimentally witness quick

³Here we need to stress that by quantum speed up we mean that our approach outperforms the classical MCMC. It is understood, that while the size of the quantum computer used is small, and specifically smaller than what can be classically simulated, the advantage of our algorithm can be viewed as a “quantum inspired” approach, while the true quantum advantage can be achieved when the QPU used is larger than what can be classically simulated.

¹S.A.ferguson-3@ed.ac.uk

²petros.wallden@ed.ac.uk

thermalisation of the CGQeMCMC. In both cases, the quantum computers part of CGQeMCMC is realised in an emulation environment (using classical devices – see [Appendix A](#) for details of the implementation).

Explicitly, our contributions are as follows:

- Propose a framework for applying coarse graining to the QeMCMC with the Ising model used as the test case. The framework allows the problem instance to be altered to reduce the number of qubits required and, in some cases, parallelise computation over multiple QPU.
- Numerical analysis of techniques within the CG framework through absolute spectral gap of small (up to 10) spin instances. The dependence on system size of each method is analysed, with one technique (multi-sampling with improved local groups) showing favourable scaling compared to classical techniques across different temperature ranges.
- Simulation of CGQeMCMC for larger Ising model instances up to 36 spins through the calculation of average magnetisation and analysis of convergence.
- Demonstration of quantum enhancement over classical methods in the above test cases while using only \sqrt{n} (perfectly simulated) qubits.

The paper is organised as follows: In Section 2 we give the necessary background namely, the classical MCMC algorithm, the spin glass Ising model, the problem of thermalisation and the QeMCMC of [1]. In Section 3 we propose a general framework for coarse graining the Ising model so that smaller quantum computers can be used to tackle larger instances within the CGQeMCMC and even achieve quantum advantage. We also discuss figures of merit of simple Markov chains and the difficulties in assessing thermalisation. Section 4 discusses the particular coarse grained proposal methods employed, before they are explored numerically in Section 5. Conclusion and future directions are given in Section 6.

2. Preliminaries

In this section, we introduce the classical Ising model, provide an overview of MCMC and the issue of thermalisation for difficult problem instances. We then introduce the QeMCMC which improves the thermalisation by utilizing quantum computation.

2.1. The Ising model

The archetypal test-case of random sampling algorithms such as MCMC are “spin glass” Ising models. “Glassy” due to their magnetic disorder in analogy with the positional disorder in chemical glass, such lattices are composed of spins that can exist in either states $s_i = \{1, -1\}$. The state, \mathbf{s} , composed of n spins is thus defined $\mathbf{s} = (s_1, s_2, \dots, s_n)$. Each configuration of spins $\{1, -1\}^n$ has an associated energy ($E(\mathbf{s})$), Boltzmann probability ($\mu(\mathbf{s})$) and magnetisation ($m(\mathbf{s})$) defined below:

$$E(\mathbf{s}) = - \sum_{j>k=1}^n J_{jk} s_j s_k - \sum_{j=1}^n h_j s_j \quad (1)$$

$$\mu(\mathbf{s}) = \frac{1}{Z} e^{-E(\mathbf{s})/T} \quad (2)$$

$$m(\mathbf{s}) = \frac{1}{n} \sum_{j=1}^n s_j \quad (3)$$

where h and J are the field and coupling respectively that define the Ising model instance, Z is the partition function $Z = \sum_{\mathbf{s}} e^{-E(\mathbf{s})/T}$ and T is a temperature parameter. The Boltzmann average magnetisation $\langle m \rangle_\mu = \sum_{\mathbf{s}} \mu(\mathbf{s}) m(\mathbf{s})$ is an example of an observable which can be hard to calculate due to the size of the state space. For just 100 spins, the number of possible configurations are $2^{100} \approx 10^{30}$ and requiring an algorithm to sum over these becomes intractable.

For systems where J and h are unstructured and have values of varying signs, the energy landscape is particularly rugged and hard to explore. When one wishes compute the value of an observable from this landscape, in the low temperature limit, very few states of low energy contribute. These states are often very far apart in Hamming distance⁴, meaning that transitioning between them proportionally to their Boltzmann probability is extremely inefficient.

2.2. Markov Chain Monte Carlo

The MCMC has a remarkable history. Named as one of the ten most influential algorithms in history, it was developed to calculate observables of a probability distribution that is too highly dimensional to be evaluated analytically or with brute force numerics [8]. The first component is the Markov chain - a walk on such a highly dimensional landscape - where the probability of each step only depends on the last position. The chain is normally produced by the Metropolis-Hastings algorithm which, with some probability (hence “Monte-Carlo”), rejects or accepts update steps based on the value of the probability distribution at that point [9, 10].

MCMC is able to skirt the responsibility of ever directly calculating the expensive (due to calculation of Z) $\mu(\mathbf{s})$. Instead, it performs an approximation by exploring the state space by random walk from an arbitrary starting point. Each step in the algorithm is composed of two sub-steps: proposal and acceptance. The *proposal* step determines the probability of state \mathbf{s}' being proposed when the system is in state \mathbf{s} . It is represented by the matrix $Q(\mathbf{s}'|\mathbf{s})$ and can be constructed in many different ways including through the use of a quantum computer as we see in Section 2.4. The *acceptance* step is often governed by Metropolis-Hastings (MH), where the matrix $A(\mathbf{s}'|\mathbf{s})$ (Equation 4) dictates the probability that a move is accepted [11, 9].

$$A(\mathbf{s}' | \mathbf{s}) = \min \left(1, \frac{\mu(\mathbf{s}')}{\mu(\mathbf{s})} \frac{Q(\mathbf{s} | \mathbf{s}')}{Q(\mathbf{s}' | \mathbf{s})} \right) \quad (4)$$

⁴Here, Hamming distance between two states is defined as the number of positions that the two states have different spin values.

Thus, the algorithm is able to explore a complicated state space by proposing a new state to move to, and moving to that state if it is of lower energy. Of course, the Markov chain can also move to states of higher energy with probability defined by Equation 4. Pseudo code is provided in Algorithm 1.

Algorithm 1: MCMC

```

// Initialisation
1  $\mathbf{s} \leftarrow$  initial spin configuration;
2 while not converged do
    // Proposal step
3    $\mathbf{s}' \leftarrow$  update proposal;
    // Classical MH accept or reject
4    $A(\mathbf{s}' | \mathbf{s}) = \min\left(1, \frac{\mu(\mathbf{s}') Q(\mathbf{s}|\mathbf{s}')}{\mu(\mathbf{s}) Q(\mathbf{s}'|\mathbf{s})}\right)$ 
5   if  $A \geq \text{random.uniform}(0, 1)$  then
6      $\mathbf{s} = \mathbf{s}'$ ;

```

The importance of the acceptance step underlies any future algorithm. One does not need to calculate $\mu(\mathbf{s})$ or $\mu(\mathbf{s}')$ at each step, merely their ratio which can be computed in $O(n^2)$ polynomial time [9]. Together, proposal and acceptance steps result in the probability matrix, $P(\mathbf{s}' | \mathbf{s}) = A(\mathbf{s}' | \mathbf{s}) Q(\mathbf{s}' | \mathbf{s})$, which is the probability that each step in the algorithm will result in transition from \mathbf{s} to \mathbf{s}' .

To ensure convergence, the Markov chain must be irreducible and aperiodic meaning that any state can be (eventually) reached from any other state and that there exists no repeating loops in the chain. Detailed balance ensures both by requiring the following is satisfied for any transition $\mathbf{s} \rightarrow \mathbf{s}'$.

$$\mu(\mathbf{s})P(\mathbf{s}|\mathbf{s}') = \mu(\mathbf{s}')P(\mathbf{s}'|\mathbf{s}) \quad (5)$$

In this context, the probability distribution $\mu(\mathbf{s})$ is often labeled as the “stationary” or “target” distribution. When the temperature drops the exponential term in the Boltzmann distribution becomes increasingly sensitive to small differences in energy levels. Consequently, the acceptance probability for proposed transitions becomes negligible, leading to extremely slow exploration of the state space. This phenomenon impedes efficient sampling and hinders convergence, as only proposals of similar or lower energy are consistently accepted. This means the Markov-chain in a relatively low energy state lies dormant until it happens across one of only a few low energy states, which takes exponential time. The QeMCMC aims to address this issue as explored in Section 2.4.

2.3. Thermalisation

Upon initialisation, the Markov-chain proceeds until thermalisation is achieved, signifying convergence to the stationary distribution. Subsequently, one can then sample from the chain at intervals spaced to ensure uncorrelated samples which is called the auto-correlation time of the Markov Chain. The expectation value of observables, such as magnetisation, can then be estimated from these non-correlated samples. However, the crux lies in thermalisation. A *local* proposal method, altering

one spin at a time, tends to get trapped in local minima. Conversely, a *uniform* random proposal explores the energy landscape inefficiently, being entirely non-local. In the low temperature regime, both approaches exhibit slow auto-correlation and thermalisation times. It should be noted that the uniform distribution will faithfully converge in a number of steps similar to that of the size of the entire state space. In other words, given the time it would take to solve the problem by brute force, the uniform proposal can approximate the solution. Thus, the uniform proposal provides an upper bound to the possible thermalisation times of MCMC.

One of the issues with thermalisation regards how one can tell when a Markov chain has reached the stationary distribution, and how many steps to take as auto-correlation time. Multiple techniques have been proposed, however many are deemed to be fickle or flawed [12, 13, 14]. For example, it is possible for two different chains on the same problem instance to both individually appear like they have converged - their observables appear stable. When they are compared side by side however, it is clear they they have “converged” to different local distributions as the observables calculated from sampling the chains are completely different [15]. Alternatively, two chains may agree on observables while neither seeming to be in a stationary distribution. The former is a particular problem when updates are particularly local.

Classical techniques such as parallel tempering or population annealing sample multiple different chains, allowing one to parallelise computation and mitigate for the issues of convergence with local proposals [16, 17, 18, 19]. These techniques are all directly applicable to CGQeMCMC, meaning any gain in convergence is propagated easily to state of the art techniques.

2.4. Quantum enhancement

Recently, the QeMCMC has extended the classical MCMC to a Noisy Intermediate Scale Quantum (NISQ) computing setting, with a cubic reduction in MCMC thermalisation time for some problems [1]. In QeMCMC, the proposal states of the Markov chain are the outcome of a quantum computation, with speedup derived from reducing the number of required update steps. The first step is to encode the current state of the Markov Chain as binary input to the computational basis state of the quantum computer - mapping the $\{1, -1\}^n$ spin states to $\{1, 0\}^n$ computational basis states. One then evolves this state according to a Hamiltonian (H).

$$H = (1 - \gamma)\alpha H_{\text{prob}} + \gamma H_{\text{mix}} \quad (6)$$

This unitary evolution takes the form: $U = e^{-iHt}$ with practical implementation requiring an approximation through the Trotter-Suzuki product. The problem Hamiltonian (H_{prob}) encodes the classical model instance and although the mixing Hamiltonian could take many different forms, it is defined here as⁵ $H_{\text{mix}} = \sum_{j=1}^n X_j$. Here, hyper-parameters are sampled in the

⁵The notation is kept in line with previous literature on the subject where possible [1, 7]

range $t = (2, 20)$ and $\gamma = (0.25, 0.6)$, although optimisation of these parameters is an ongoing issue.

$$H_{\text{prob}} = - \sum_{j>k=1}^n J_{jk} Z_j Z_k - \sum_{j=1}^n h_j Z_j = \sum_{\mathbf{s}} E(\mathbf{s}) |\mathbf{s}\rangle \langle \mathbf{s}| \quad (7)$$

Measurement in the computational basis state returns a binary outcome that is used as the proposal state as seen in Algorithm 2. The Hamiltonian is inspired by the adiabatic program, and perturbative analysis expects it to propose states similar in energy to the previous state, and far in Hamming distance[1]. Both of these properties are optimal for fast MCMC convergence rate, and cannot be replicated using classical computers. Other choices of unitary evolution have been proposed to replace the time-independent Hamiltonian evolution, however these have not yet been explored experimentally and thus wont be considered here [20].

Algorithm 2: QeMCMC proposal step

```
// Initialisation
1  $\mathbf{s} \leftarrow$  initial spin configuration;
// Quantum proposal step
2  $\gamma \leftarrow$  hyper-parameter in range (0.25, 0.6) ;
3  $t \leftarrow$  hyper-parameter in range (2, 20);
// quantum computation
4  $|\psi\rangle = \exp[-iHt]|\mathbf{s}\rangle$  ;
5  $\mathbf{s}' = \text{X measurement result of } |\psi\rangle$  ;
```

The quantum proposal distribution, $Q(\mathbf{s}' | \mathbf{s}) = |\langle \mathbf{s}' | U | \mathbf{s} \rangle|$, has the symmetry requirement: $|\langle \mathbf{s} | U | \mathbf{s}' \rangle| = |\langle \mathbf{s}' | U | \mathbf{s} \rangle|^2$. Normally, one is required to calculate $Q(\mathbf{s}' | \mathbf{s})$ explicitly as in Equation 4, however as it is merely the ratio of $\frac{Q(\mathbf{s}' | \mathbf{s})}{Q(\mathbf{s} | \mathbf{s}')}$ required, the equation easily simplifies thanks to the symmetry constraint.

$$Q(\mathbf{s}' | \mathbf{s}) = |\langle \mathbf{s}' | U | \mathbf{s} \rangle|^2 = |\langle \mathbf{s} | U | \mathbf{s}' \rangle|^2 = Q(\mathbf{s} | \mathbf{s}') \quad (8)$$

This reduces the Metropolis method (Equation 4) to:

$$A(\mathbf{s}' | \mathbf{s}) = \min\left(1, \frac{\mu(\mathbf{s}')}{\mu(\mathbf{s})}\right) = \min\left(1, \exp\frac{E(\mathbf{s}) - E(\mathbf{s}')}{T}\right) \quad (9)$$

Of course, this elegant simplification of the Metropolis acceptance criteria is not enough to suggest quantum advantage. Both perturbation theory and numerical analysis have shown that a quantum update as above have some remarkable properties [1]. Proposals that maximise the Hamming distance between \mathbf{s} and \mathbf{s}' (as in the uniform update) while minimising the Energy difference (as in the local update) and are thus likely to be accepted are optimal. This is exactly the criteria that the QeMCMC meets, meaning it has freedom of movement on the lattice at no cost to acceptance probability. One can view this advantage as “searching” over a superposition of possible states of similar energy, before collapsing to one at measurement. This becomes incredibly important when in the low temperature regime. As mentioned in Section 2.2, Markov-chain suffer

from low acceptance rate in the low temperature regime so proposals that can suggest similar energy states are highly likely to be accepted and can significantly improve a Markov-chains convergence.

3. Framework and figures of merit

In this section, we establish the foundational framework for employing CGQeMCMC techniques on the Ising model by outlining the key components and methodologies. Additionally, we provide a comprehensive overview of two pivotal figures of merit: the absolute spectral gap and magnetisation estimation. These metrics are introduced to provide background for the numerical experiments detailed in Section 5.

3.1. Framework

In CG modelling, the behaviour of a complex system is simulated by using a simpler representation of the system. This is immediately realised in Ising models at each MCMC step by isolating a group consisting of q spins - here referred to by the corresponding fraction of the lattice per group (q/n). These spins may not necessarily be close to one another or even interact, however the optimal (in terms of thermalisation) choice of spins in a group is likely to depend on the details of the problem. The coarse graining is shown in Algorithm 3, where the QeMCMC (Algorithm 2) is run as a subroutine on a small group s_g .

Algorithm 3: Coarse Graining

```
1  $\mathbf{s} \leftarrow$  initial spin configuration;
2  $q \leftarrow$  size of group;
3  $\mathbf{s}' \leftarrow \mathbf{s}$ 
4  $index \leftarrow$  find spins in group;
5  $s_g \leftarrow$  subset of  $s$  using  $index$ ;
// Do QeMCMC subroutine, Algorithm 2
6  $s'_g \leftarrow$  QeMCMC ( $s_g$ );
// update  $\mathbf{s}'$  with results from  $s'_g$  QeMCMC
7  $\mathbf{s}'[index] \leftarrow s'_g$  ;
```

Of course, there is scope for a multitude of different groupings, sub-groupings and clusterings as is sometimes seen in classical literature [21, 22, 23, 24, 25, 26]. These are not exhaustively discussed here, where we simply give the framework of coarse graining the Ising model lattice along with some illustrative examples that demonstrate the potential of the approach. Discussion of the choice of spins to include in the active group, as well as the parameters chosen as input to the QeMCMC, including the choice of the “reduced” Hamiltonian, are left to Section 4. It should be made clear that any Quantum enhancement found can most likely be combined with traditional MCMC methods in hybrid schemes that are likely to outpace “plain” MCMC, regardless of proposal.

3.2. Spectral Gap

As mentioned in Section 2.3, estimating the thermalisation time (τ_ε) of an algorithm is not simple, as one cannot necessarily tell when the Markov chain is in the stationary state. There is also a dependence on the starting state of the algorithm meaning between successive MCMC runs thermalisation can differ in steps by orders of magnitude. The thermalisation time is however bounded analytically:

$$(\delta^{-1} - 1) \ln\left(\frac{1}{2\varepsilon}\right) \leq \tau_\varepsilon \leq \delta^{-1} \ln\left(\frac{1}{\varepsilon \min_s \mu(s)}\right), \quad (10)$$

where ε is the error in total variational distance used to quantify the bounds of (τ_ε) [27]. The Spectral gap (δ) describes the slowest facet of a chains convergence and is found through the transition probability matrix, P . Given the eigenvalues $\{\lambda\}$ of P , δ is calculated:

$$\delta = 1 - \max_{\lambda \neq 1} |\lambda| \quad (11)$$

The Spectral gap is inversely proportional to the upper bound of the thermalisation time (Equation 10) and thus provides an unambiguous quantification of a Markov chains convergence. Numerical calculation of δ is very inefficient however, requiring numerical integration (often by random sampling, see Appendix A) to create the ($2^n \times 2^n$) P matrix before Eigen-decomposition. Due to this, calculation of the spectral gap is exponentially more demanding than an actual MCMC algorithm.

The spectral gap also ignores the use of a particular chain in more sophisticated schemes mentioned in Section 2.3 that rely on running multiple chains concurrently. Thus, one must be reluctant to overstate the results of spectral gap analysis.

3.3. Convergence analysis

To analyse the convergence of CGQeMCMC in test cases that is currently technologically inaccessible to QeMCMC, we run Markov Chains and estimate the average magnetisation and energy of the Boltzmann distribution. For low temperatures, this essentially becomes an optimisation problem as only a few states contribute.

As mentioned in Section 2, calculating the average magnetisation $\langle m \rangle_\mu$ is dependent on first calculating the partition function. This makes direct calculation infeasible for even relatively simple systems. The alternative is to perform the following estimation where $m(s)$ is calculated for each sampled state by Equation 3:

$$\langle m \rangle_\mu \approx \frac{1}{N} \sum_{s \in S} m(s) \quad (12)$$

Assuming thermalisation of the Markov chain, this is accurate with high probability even when N is very small in comparison to the entire state space [28, 27]. One can use estimation of this observable as a figure of merit by asking the question: “How well can our Markov chain estimate the true magnetisation?”. Of course this requires knowledge of the stationary distribution. Here the stationary distribution of exemplar 16, 25

and 36 spin instances are found by brute force, meaning that the update proposals can be evaluated against the true magnetisation as benchmark.

Specifically, this paper will look at cumulative magnetisation as sampling from Markov Chains generally requires thinning (to take non-correlated samples) and burning (to ensure thermalisation) which incurs hyper-parameters complicating the analysis.

Crucially, in certain cases, magnetisation estimation can be a flawed figure of merit. As briefly discussed in Section 2.3, a chain may appear to converge to the stationary distribution, while it is actually stuck in a local minimum. If the magnetisation contribution of this local minimum is similar to that of the actual magnetisation, then this becomes a flawed figure of merit. Thus, alongside the magnetisation calculation we analyse the convergence of average energy between multiple chains which can be compared with the exact average energy for the stationary distribution. If local minima impede convergence, this measure will display an obvious bias.

4. Coarse graining strategies

In this section, we give three different coarse graining strategies: (a) a “naive” approach where one chooses a random subset of spins and ignores the rest, (b) an improved local approach where one chooses a random subset of spins while treating the remaining spins as an external field and (c) an approach that one considers multiple subsets, treating each of them separately as in the earlier approaches.

Before proceeding to the proposed strategies, let us highlight two properties of the QeMCMC method that were key to the advantage demonstrated in [1]. The first is that the Hamiltonian used (evolution to obtain the proposal step) includes the problem’s Hamiltonian, and with suitable choice of parameters the proposal step does not differ significantly in energy – thus ensuring proposed steps that are accepted even when being close to thermalisation. The second is that, unlike classical local strategies, QeMCMC can lead to proposal step that differs (significantly) in Hamming distance from the previous step, “spanning/searching” the full space and escaping from local minima.

4.1. Naive CG - local groups

The naive choice of coarse graining is to pick spins that are neighbours forming a *local group*, $g_l = s_r, s_{r+1} \dots s_{r+q}$ where s_r is a randomly selected spin that begins the group⁶. Once isolated, the group is updated according to the QeMCMC routine outlined in Section 2.4 with \tilde{J} and \tilde{h} the parameters defining the “partial Hamiltonian” of the newly formed group. This new Hamiltonian essentially ignores the spins not selected:

⁶We need to stress here that the spins and their “locality” refers to their labels, that in some cases (e.g. 1-d Ising model) also carry physical information, while in other cases (random Ising model) do not. We still use the term “local” to distinguish this coarse graining strategy from others, but we want to make sure that this is not mistakenly understood as “physically” local.

$$\tilde{J} = J_{i \in g_l, j \in g_l}, \tilde{h} = h_{i \in g_l} \quad (13)$$

Ignoring the surrounding spins is an approximation that understandably has limitations and specifically raises two main issues. Firstly, the Hamming distance of proposal steps is fundamentally restricted to the size of the group. While this is better than classical local move approaches, it still puts a bound on the jumps that the proposal steps can make, and is more likely to get stuck in local minima (as with the classical local proposal) and partially cancels one of the key properties that lead to the success of the QeMCMC - namely the large Hamming distance update proposals.

The second issue is that the new problem Hamiltonian H'_{prob} is missing contributions from the ignored spins making the evolution fundamentally incomplete. This partly cancels the other advantage of QeMCMC highlighted earlier, that it includes the problem's Hamiltonian. If one were to consider a 1D Ising model where only neighboring spins interact, this choice of CG is likely to perform adequately, as the boundary interaction terms of the group is constant (2) with cluster size, meaning the impact of missing contributions from ignored spins scales favourably with group size. The same is not true for general Ising models with higher connectivity.

To sum-up, this CG shares some of the advantages of QeMCMC: can “tunnel” through local minima (but with limitations on the width due to the bound on the Hamming distance that the proposal step can make); has some information of the problem Hamiltonian (but misses important information for general Ising Hamiltonians).

4.2. Improved local groups

Motivation: As we have seen above, the local groups CG becomes increasingly inaccurate when considering Hamiltonians with high connectivity, since the contributions from the “ignored” spins become more relevant. An important observation, however, is that the non-selected spins are constant with respect to the selected ones, and we could treat their interaction energy as a field.

Explicitly, the interaction matrix is the same as in the local grouping, $\tilde{J} = J_{i \in g_l, j \in g_l}$, but the non-selected spins are treated as environment, adding them to the field of the i^{th} selected spin as:

$$\tilde{h}_i = h_i + \sum_{j \notin g_l}^n J_{ij} s_j \quad (14)$$

In this way, the accuracy of the Hamiltonian is increased from the local group method without the addition of any quantum gates. The effective Hamiltonian H'_{prob} now fully represents the *relative* energy of any two states of the group. As will become clear in Section 5, improved local grouping refines the naive local groups, however there is still tail-off for small q/n .

Overall, this *Improved* local group method can tunnel through local minima with the same Hamming distance limitations as the local grouping, but now contains a much more accurate representation of the problem Hamiltonian.

4.3. Multiple groups

Motivation: To mitigate the issue of low Hamming distance proposals, one can evaluate multiple local groups in a single step meaning the one-shot QeMCMC becomes a succession of single shots of multiple local groups.

Algorithm 4: CGQeMCMC subroutine

```

// Initialisation
1  $\mathbf{s} \leftarrow$  initial spin configuration;
2  $n_g \leftarrow$  number of groups;
3  $l_g \leftarrow$  size of group;
4  $\mathbf{s}' \leftarrow \mathbf{s}$ ;
5 for  $i \leftarrow 0$  to  $n_g$  do
6    $index \leftarrow$  spins in  $i^{th}$  group;
7    $s_g \leftarrow$  subset of  $\mathbf{s}$  using  $index$ ;
   // Do QeMCMC subroutine, Algorithm 2
8    $s'_g \leftarrow$  QeMCMC( $s_g$ );
   // update  $\mathbf{s}'$  with results from  $i^{th}$  group's
   QeMCMC
9    $\mathbf{s}'[index] \leftarrow s'_g$ ;

```

Essentially, instead of taking just one local group of spins, we evaluate multiple (disjoint) groups, each individually. While there are many such strategies, we choose a simple one that reduces asymptotically the size of QPU required: we use \sqrt{n} groups of size \sqrt{n} . This method can be easily combined with the improved local group method resulting in an iterative process that loops through the entire lattice where each quantum computation inherits the measurement results of the last.

Explicitly, we first split the spins into our \sqrt{n} local groups before evaluating the first group individually using the Improved local group method. The measurement results of this group then update the state of the system, impacting the environment of the next group which is subsequently evaluated using the Improved local method. In this way, our algorithm iterates through the groups, where at each step the measurement results update the system for subsequent groups' update. The MH acceptance is only computed after the entire state has been updated by each of the \sqrt{n} groups. For the remainder of the paper, this method will be labeled “multiple sampling” and will harness the Improved local group strategy.

With this CG we are able to maintain both advantages of QeMCMC described at the start of the section: can jump to arbitrary Hamming distances; use the full problem Hamiltonian for these jumps.

5. Numerical Results

In this section we analyse the results of our numerical experiments of Ising model CGeMCMC, while further details of the implementation can be found in [Appendix A](#).

5.1. Spectral gap

To quantify the CGQeMCMC, the effect of reducing q on the convergence of the resulting Markov chain must be understood,

with the particular aim of understanding the different coarse grained proposals at $q = \sqrt{n}$. This is done by evaluating the spectral gap of the CG methods for randomly initialised fully-connected Ising models in the range 4 – 10 spins. Figure 1 shows the decrease of spectral gap with q/n for each of the CG methods and $n = \{6, 8, 10\}$. Clearly the decay is worse for techniques that do not multiple sample, suggesting that the locality of low q restricts the proposal. This effect is dependent on system size, however it is difficult to quantify using only the small systems at our disposal. There is also a temperature dependence, as the performance of small q is inextricably linked with the performance of the classical local proposal. For analysis of temperature dependence for a 9 spin instance see Figure 2.

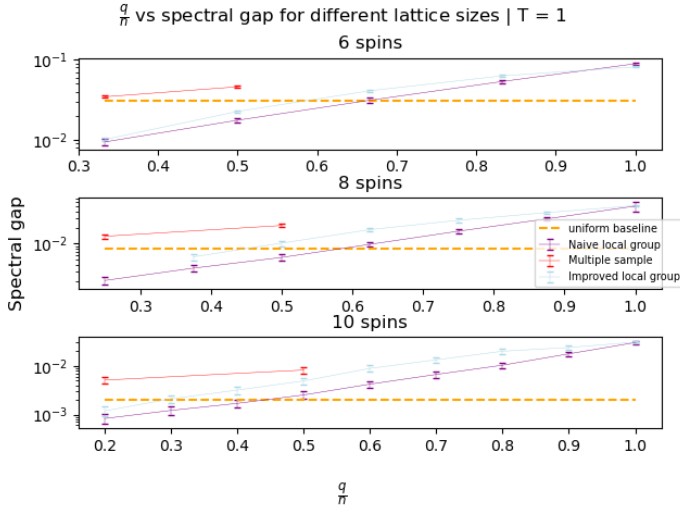


Figure 1: Spectral gap with q/n for $n = 6, 8, 10$, with classical uniform benchmark in orange. Naive local group (purple) is seen to perform badly as q is decreased, while using an improved local group (light blue) performs significantly better. Multiple sampling with Improved local groups (red) is seen to perform considerably better than both, however the existence of few very factors of small numbers limits proper analysis. Note that the logarithmic scale on the y-axis varies between subplots.

In order to assess how the multiple sample technique fares, one must be careful. A silent parameter here is the remainder of integer division in q/n . If we have $n = 10$ and $q = 6$, the remainder is 4, meaning an optimal multiple sample strategy with $q = 6$ also has another 4 qubit quantum computation. As this is an effect that is negligible at large n , we avoid this complication by finding the two closest integer values to $q = \sqrt{n}$ and interpolating to estimate the spectral gap value. The interpolation is linear, with errors propagated from the error in spectral gap of the two neighbouring points. The linear assumption is likely to underestimate the true value. Of course, for 4 and 9 spins interpolation is not required.

In analogy with [1] Figure 2a, the different update proposal strategies are compared for a representative set of 100 randomly initialised 9 spin fully-connected Ising model instances in Figure 2. The QeMCMC (blue) is far superior to any classical strategy (orange and green) in the low temperature regime. The CGQeMCMC with 3 groups of 3 qubits (red) is also superior to

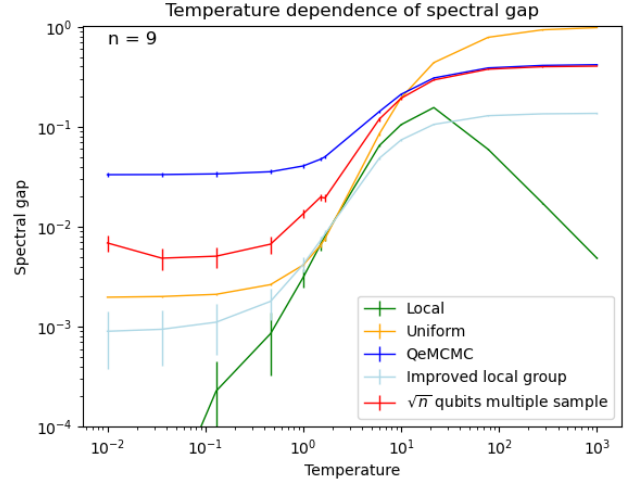


Figure 2: Spectral gap varying with temperature for 100 randomly initialised 9 spin fully-connected Ising model. The classical uniform (orange) and local (green) strategies are clearly improved at low temperatures by the QeMCMC strategy (blue) [1]. The red data represents CGQeMCMC with $q = \sqrt{n} = 3 = n_g$ (3 groups of 3 spins). The light blue data is $q = \sqrt{n}$ but $n_g = 1$ (1 group of 3 spins).

the classical strategy, however the speedup is clearly dampened. If one evaluates a single 3 spin group on the lattice each quantum proposal (transparent blue) the quantum speedup is lost for most temperature ranges for this system size.

There is evident promise of quantum speedup using merely \sqrt{n} qubits, however speedup at a fixed system size is less important. The scaling behaviour of the proposal step is necessarily analysed at $T = 1$ in Figure 3. Equation 15 is the exponential fitting function used in the figures, where a small k represents good scaling of a proposal strategy. The data points for larger systems are less reliable due to a much restricted sample size (50) for the average spectral gap. This leads to added uncertainty in the fits, and increased reliance on the convergence analysis in Section 5.2.

$$\delta = a \times 2^{-kn} \quad (15)$$

In Figure 3, the classical uniform and local proposals perform poorly, with $k = 0.97(1)$, $0.92(4)$ respectively. The coarse grained quantum proposals perform considerably better, in particular the multiple sample proposal with $k = 0.50(3)$. The average quantum enhancement factor (k_{QEF}) is the ratio of k for the quantum algorithm and the k from the best classical proposal:

$$k_{QEF} = \frac{k_{classical}}{k_{quantum}} \quad (16)$$

For the multiple sample proposal strategy, we see a quantum enhancement factor of $k_{QEF} = 1.84$ against the best classical approach - the local proposal. In this data, the QeMCMC gains an enhancement of 2.7, a slightly reduced value than reported in [1] for the same temperature. Figure 3 depends largely on the temperature while Figure 2 depends on the problem size.

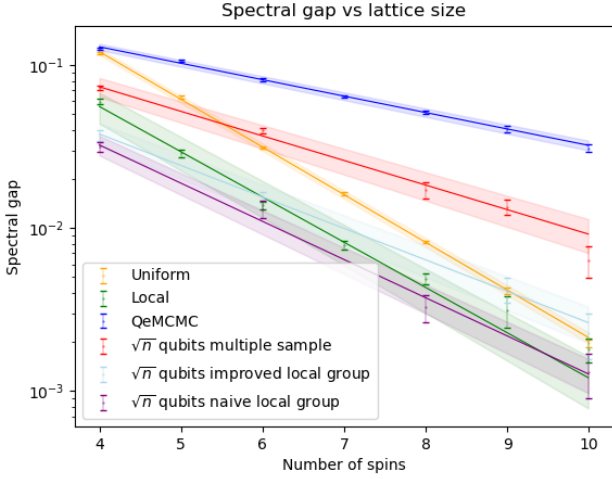


Figure 3: Spectral gap varying with problem size for 500 randomly initialised fully-connected Ising models of each integer number of spins. Only 50 systems of 9 and 10 spins for CG techniques were evaluated due to computational limitations. Each data set has least squares exponential fits with fitting function Equation 15. As the system size increases, the spectral gap of classical uniform (orange) and local (green) strategies clearly decrease faster than those of the QeMCMC (blue) and CGQeMCMC (red, light blue) proposals. For a given proposal, the value of k determined by best fit is as follows: Uniform: 0.97(1), Local 0.92(4), QeMCMC: 0.335(8), local group: 0.77(2), Improved local group: 0.64(2), multiple sample: 0.50(3). k values for $T = 0.1$ and $T = 10$ are listed in appendix B.1 alongside the appropriate figures.

Appendix B provides multiple figures that explores these relations. The corresponding quantum speedups in k for $T = 0.1$ and $T = 10$ are 2.17 and 2.6 respectively. Of course, the problem instance type (1D, 2D, fully connected, sparse etc.) influences the outcome of these experiments, however these topics are beyond the scope of this work.

Figure 3 may wrongly suggest that the uniform proposal is a useful step. In practice, the local proposal is much more useful in the classical schemes such as parallel tempering mentioned earlier. Any quantum proposal step, particularly when the Hamming distance of steps has been reduced by CG, will be useful in much the same way that the local step is in practice.

5.2. Convergence analysis

Markov chains using local, uniform and CGQeMCMC are used to evaluate the average energy and magnetisation of the stationary distribution of exemplar fully-connected Ising models. Systems of size 16, 25 and 36 (see Appendix B for 15 and 36 spin results) are the focus so that \sqrt{n} qubits can be easily compared with classical methods. The stationary distribution of the 25 spin instance at $T = 1$ is primarily composed of just a few low energy states. The Boltzmann probabilities of the ground state and 1st - 3rd excited states are: 68.6%, 25.4%, 4.2%, 0.5%. If one were to sample lower temperature distributions the problem essentially becomes one of optimisation, while at higher energy the problem becomes less difficult as one transitions from the ferromagnetic phase. See Appendix B for temperature and system size analysis.

Figure 4 shows the effective convergence of CGQeMCMC, however it is clear that the problem of getting stuck in local minima is inherited as the average energy over 10 Markov chains is biased by a few that have not found the minimum state. One can crudely evaluate convergence in this relatively low temperature regime by calculating how many chains have discovered the minimum state. In this example, of the 10 chains for each proposal, 4 local chains, 2 uniform chains and 5 CGQeMCMC have found the minima. Considering the classical methods had an extra order of magnitude (due to computational limitations) to search the state space, it is clear that quantum proposal is considerably more efficient. It should be noted that to evaluate this system by brute force requires $\approx 3 \times 10^7$ samples, meaning that the uniform proposal does not provide a practically useful proposal method, merely an upper bound on optimal thermalisation.

Analysis of the average cumulative magnetisation in Figure 5 *incorrectly* suggest that the classical local proposal converges particularly well, however further analysis (including Figure 4) suggests that local minima of similar magnetism to the global minima are contributing to no observable bias in the magnetisation. The CGQeMCMC does however observe a bias, due to some chains being stuck in local minima with different magnetisation. In the 25 spin example, the 4th excited state has a large Hamming distance from any other low energy state, being 12 spin flips from any of the other lowest 10 states. This is a very large Hamming distance, so traversing the energy landscape from the local minima is very difficult. Although any local proposal is likely to over-sample this region, the magnetisation of this state is the same as the ground state, meaning that this is not picked up in average magnetisation. This leads one to conclude that cumulative average magnetisation is not sufficient to fully characterise the thermalisation of a Markov chain.

As only one model was considered for each system size and the average magnetisation provides biased results in this instance, no explicit results are reported from this section. It is clear however that even when only employing 5 simulated qubits, a quantum enhanced search of the state space is more effective than both classical methods.

6. Conclusions

In this paper starting with the QeMCMC approach of [1], we identified two important elements that lead to its desirable performance, namely the possibility to suggest proposal steps with big Hamming distance from the previous configuration (due to generating superposition of all configurations), while returning a new configuration that is close in energy with the previous one (due to the use of the problem Hamiltonian and the suitable annealing-style brief evolution). At the same time we identified, as a limitation of QeMCMC, the necessity for using QPUs of size as large as the Ising system considered.

In order to enable the use of small QPUs we introduced the concept of coarse graining, meaning that we considered a subset of the overall system in order to find the next suggested configuration. To make our proposal competitive with QeMCMC and

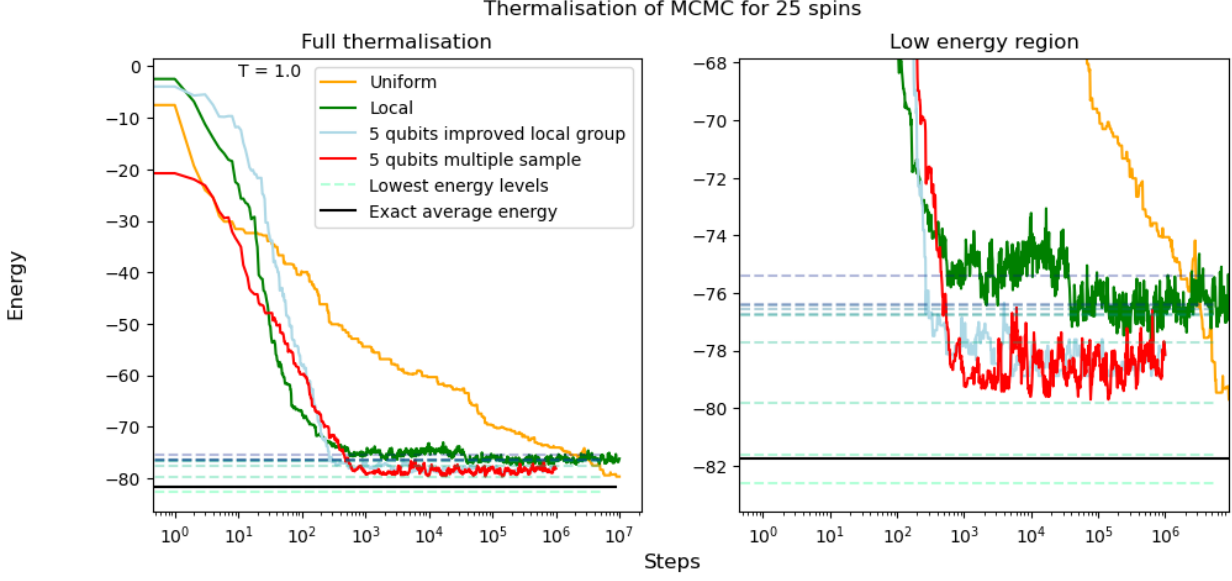


Figure 4: Average energy of 10 chains for uniform (orange), local (green), Improved local group (light blue) and multiple sample (red) with $q = \sqrt{n} = 5 = n_g$ (5 groups of 5 spins) for $T = 1$. Right figure is close-up of the low energy region. The classical local proposal has a large offset from the true average energy (black line). This is greatly reduced by CGQeMCMC. The uniform proposal suffers from extremely slow convergence but does not get stuck in local minima.

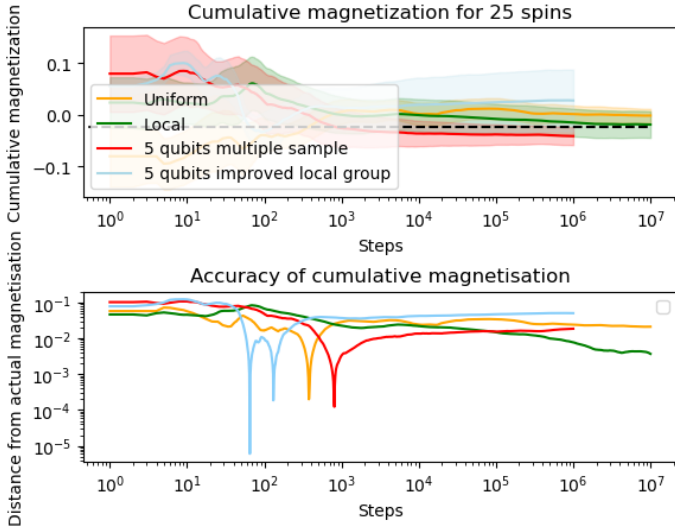


Figure 5: Cumulative magnetisation (top) of 10 chains for uniform (orange), local (dark green) and CGQeMCMC (light green) with $q = \sqrt{n} = 5 = n_g$ (5 groups of 5 spins) for $T = 1$. The accuracy of average magnetism (bottom) compared to the actual value calculated by brute force erroneously suggests that the classical local has converged.

classical solutions, we aimed to find a coarse graining that retains (largely) the two advantages of QeMCMC. Our final “multiple groups” coarse graining achieves this: can give rise to new configurations that differ as much in Hamming distance as one wishes; for each “local” subpart considered we used an effective reduced Hamiltonian that treats the coarse grained spins as an external field, achieving a sufficiently good approximation.

We then tested our proposal(s) using two figures of merit: The absolute spectral gap and magnetisation estimation. Spectral gap analysis of simulated quantum proposals in Section 5.1 was confined to systems comprising 10 spins or fewer. Nevertheless, the observed scalability of CGQeMCMC proposals relative to system size shows promising trends. Using only \sqrt{n} qubits, Quantum-enhanced Markov Chain thermalisation is predicted to outperform classical techniques for larger systems, giving a quantum enhancement factor k_{QEF} (see Section 5.1 and Equation 16 specifically) between 1.84 and 2.6.

The Markov Chain Monte Carlo algorithm was then executed in order to estimate the magnetisation for larger systems up to 36 spins, with coarse grained quantum proposals again using only \sqrt{n} simulated qubits. Both classical proposals analysed here (local and uniform) struggle to reach thermalisation in these larger systems, falling into local minima or inefficiently exploring the large state-space. The coarse grained quantum proposals improve convergence overall for these larger systems, however they also occasionally suffer from local minima.

There are many directions for future investigations related to the CGQeMCMC. The choice of $q = \sqrt{n}$ qubits in this paper was successful, however the optimal relation between q and fastest thermalisation or indeed auto-correlation remains open. Likewise, the effect of noise has not been investigated. The QeMCMC method is by construction noise-resilient, and our

CG approach uses smaller QPUs minimising further these effects, but still concrete analysis for the level and types of noise that can be accommodated maintaining the quantum advantage is another open question. Here it is also worth pointing out that due to the one-shot nature of the algorithm, standard error mitigation methods would fail and it would require a bespoke scheme that is outwith current literature [29, 30].

An important future step is to apply coarse graining to problems other than the Ising model. Application of variationally prepared Hamiltonian evolution is also an interesting avenue of research, as is coarse graining quantum algorithms that have already been derived from the QeMCMC [6, 7]. Other interesting next steps are to apply the CGQeMCMC to quantumly enhance classical methods such as simulated annealing, parallel tempering and population annealing.

Acknowledgements

PW acknowledges support by EPSRC grants EP/T001062/1, EP/X026167/1 and EP/T026715/1, STFC grant ST/W006537/1 and Edinburgh-Rice Strategic Collaboration Awards and SF acknowledges support by EPSRC DTP studentship grant EP/W524311/1.

References

- [1] D. Layden, G. Mazzola, R. V. Mishmash, M. Motta, P. Wocjan, J.-S. Kim, S. Sheldon, Quantum-enhanced markov chain monte carlo, *Nature* 619 (7969) (2023) 282–287.
- [2] C. J. Geyer, Practical markov chain monte carlo, *Statistical science* (1992) 473–483.
- [3] S. Duane, A. D. Kennedy, B. J. Pendleton, D. Roweth, Hybrid monte carlo, *Physics letters B* 195 (2) (1987) 216–222.
- [4] S. Brooks, A. Gelman, G. Jones, X.-L. Meng, *Handbook of markov chain monte carlo*, CRC press, 2011.
- [5] A. Montanaro, Quantum speedup of monte carlo methods, *Proceedings of the Royal Society A: Mathematical, Physical and Engineering Sciences* 471 (2181) (2015) 20150301.
- [6] O. Lockwood, P. Weiss, F. Aronshtein, G. Verdon, Quantum dynamical hamiltonian monte carlo, *arXiv preprint arXiv:2403.01775* (2024).
- [7] Y. Nakano, H. Hakoshima, K. Mitarai, K. Fujii, Qaoa-mc: Markov chain monte carlo enhanced by quantum alternating operator ansatz, *arXiv preprint arXiv:2305.08789* (2023).
- [8] J. Dongarra, F. Sullivan, Guest editors introduction to the top 10 algorithms, *Computing in Science & Engineering* 2 (1) (2000) 22–23.
- [9] N. Metropolis, A. W. Rosenbluth, M. N. Rosenbluth, A. H. Teller, E. Teller, Equation of state calculations by fast computing machines, *The journal of chemical physics* 21 (6) (1953) 1087–1092.
- [10] G. Fishman, *Monte Carlo: concepts, algorithms, and applications*, Springer Science & Business Media, 2013.
- [11] W. K. Hastings, Monte carlo sampling methods using markov chains and their applications (1970).
- [12] A. Vehtari, A. Gelman, D. Simpson, B. Carpenter, P.-C. Bürkner, Rank-Normalization, Folding, and Localization: An Improved \hat{R} for Assessing Convergence of MCMC (with Discussion), *Bayesian Analysis* 16 (2) (2021) 667–718.
- [13] J. M. Flegal, *Monte Carlo Standard Errors for Markov Chain Monte Carlo*, University of Minnesota, 2008.
- [14] C. J. Geyer, Introduction to markov chain monte carlo, *Handbook of markov chain monte carlo* 20116022 (2011) 45.
- [15] T. Moins, J. Arbel, A. Dutfoy, S. Girard, On the use of a local \hat{r} to improve mcmc convergence diagnostic, *Bayesian Analysis* 1 (1) (2023) 1–26.
- [16] J. Machta, R. S. Ellis, Monte carlo methods for rough free energy landscapes: Population annealing and parallel tempering, *Journal of Statistical Physics* 144 (2011) 541–553.
- [17] W. Wang, J. Machta, H. G. Katzgraber, Comparing monte carlo methods for finding ground states of ising spin glasses: Population annealing, simulated annealing, and parallel tempering, *Physical Review E* 92 (1) (2015) 013303.
- [18] M. Weigel, L. Barash, L. Shchur, W. Janke, Understanding population annealing monte carlo simulations, *Physical Review E* 103 (5) (2021) 053301.
- [19] R. H. Swendsen, J.-S. Wang, Replica monte carlo simulation of spin-glasses, *Physical review letters* 57 (21) (1986) 2607.
- [20] G. Mazzola, Sampling, rates, and reaction currents through reverse stochastic quantization on quantum computers, *Physical Review A* 104 (2) (2021) 022431.
- [21] Z. Zhu, A. J. Ochoa, H. G. Katzgraber, Efficient cluster algorithm for spin glasses in any space dimension, *Physical review letters* 115 (7) (2015) 077201.
- [22] J. Houdayer, A cluster monte carlo algorithm for 2-dimensional spin glasses, *The European Physical Journal B-Condensed Matter and Complex Systems* 22 (2001) 479–484.
- [23] U. Wolff, Collective monte carlo updating for spin systems, *Physical Review Letters* 62 (4) (1989) 361.
- [24] R. H. Swendsen, J.-S. Wang, Nonuniversal critical dynamics in monte carlo simulations, *Physical review letters* 58 (2) (1987) 86.
- [25] D. Wu, R. Rossi, G. Carleo, Unbiased monte carlo cluster updates with autoregressive neural networks, *Physical Review Research* 3 (4) (2021) L042024.
- [26] I. Murray, *Advances in Markov chain Monte Carlo methods*, University of London, University College London (United Kingdom), 2007.
- [27] D. A. Levin, Y. Peres, *Markov chains and mixing times*, Vol. 107, American Mathematical Soc., 2017.
- [28] V. Ambegaokar, M. Troyer, Estimating errors reliably in monte carlo simulations of the ehrenfest model, *American Journal of Physics* 78 (2) (2010) 150–157.
- [29] Y. Li, S. C. Benjamin, Efficient variational quantum simulator incorporating active error minimization, *Physical Review X* 7 (2) (2017) 021050.
- [30] K. Temme, S. Bravyi, J. M. Gambetta, Error mitigation for short-depth quantum circuits, *Physical review letters* 119 (18) (2017) 180509.
- [31] Y. Suzuki, Y. Kawase, Y. Masumura, Y. Hiraga, M. Nakadai, J. Chen, K. M. Nakanishi, K. Mitarai, R. Imai, S. Tamiya, et al., Qulacs: a fast and versatile quantum circuit simulator for research purpose, *Quantum* 5 (2021) 559.
- [32] S. Ferguson, *Cgqemcmc: Python repository for coarse-graining the quantum enhanced markov chain monte carlo* (2024). URL <https://github.com/Stuartferguson00/CGQeMCMC>
- [33] R. Pal, *Qumcmc: Python implementation of quantum enhanced markov chain monte carlo* (2023). URL <https://github.com/pafloxy/quMCMC>

Appendix A. Implementation details

The numerical quantum simulations were carried out using python 3.11, running qulacs quantum circuit simulator [31] and can be found open source on Github [32]. The base of the code was built upon a pre-existing library, however it was drastically modified to fit the requirements of this paper [33].

To keep consistent with the original work, parameters have been kept constant as much as possible [1]. For example, γ is varied in the range (0.25, 0.6) and the integer time parameter is varied between (2, 20) for all of the following experiments. One key difference is the method of calculating the spectral gap for quantum proposal methods. The authors of [1] employed exact numerical integration by discretising the gamma parameter. Here however, we employ Monte-Carlo integration by uniformly sampling the t and γ regions. Explicitly, this means that for a given row of the Q matrix, the measurement statistics are

estimated by averaging over 30 (a value chosen by experimentation) randomly generated t and γ values. When one is doing plain QeMCMC or CGQeMCMC without multiple groups, the i^{th} row of Q can be found by doing the following 30 times: First, randomly generate t and γ values then use as quantum input the i^{th} state, run the appropriate quantum circuit and output the statevector. Clearly, averaging over the 30 statevectors gives a good approximation of the likely transitions between states.

For CGQeMCMC however, the situation is more difficult. As the output of one circuit affects the gates of the next, then the entire Q matrix must be found by brute force. First, randomly select a starting state, run a CGQeMCMC step where t and γ are randomly chosen and then add $1/n_s$ to the $(i, j)^{th}$ element of Q . Repeating this many times leads to an accurate approximation of Q . To justify how many times is required, this process was repeated for over multiple different sample numbers with $n_s = (2^n)^2$ deemed fit.

Appendix B. Extra data

Here, extra data is included without detailed analysis for the interested reader.

Appendix B.1. Hamming distance and Energy difference of proposals

In this section, the Hamming distance and energy difference of proposed steps are compared. The classical local step will only ever take steps of Hamming distance = 1, meaning it is entirely local but has a high acceptance rate as the energy difference of proposed steps is low. This means that such updates traverse the cost function landscape in a very local way, often getting stuck in local minima for very long periods of time. The uniform proposal has the extreme opposite feature, as it picks a possible step at random, it has a very low acceptance rate meaning slow exploration of the landscape as the energy of a proposed state is unlikely to be close or lower. When a step is accepted however, the hamming distance is very large. Both of the above points are made clear in Figure B.6.

Any CG method that does not multiple sample will have the locality issue of occasionally getting stuck in minima. If one does multiple sample, it becomes clear that the Hamming distance is slightly reduced compared to the uniform or QeMCMC method. The energy difference of proposals still outperforms classical methods, almost matching the QeMCMC. One interesting artefact is that the improved local group (without multiple sampling) greatly reduces the energy difference compared to all methods, while increasing the Hamming distance compared to the classical local method. This means that if one were to choose a problem where the local method performs well (for example in particular temperature regimes) then the improved local method is always likely to sustainably outperform the classical proposals. Scaling of this artefact is left to future work.

Appendix B.2. Temperature and convergence for large systems

The relationship between temperature, system size and thermalisation is conveyed through analysis of the energy convergence in Figure B.7. One can see that the thermalisation of the uniform proposal becomes useless for large systems, the local proposal struggles at low temperatures and in every case, both quantum proposals analysed efficiently find a better than classical low energy regime. Magnetisation plots are not provided as they falsely suggest convergence of non-converged distributions.

Appendix B.3. Temperature and scaling

The temperature dependence of spectral gap scaling is briefly conveyed here through a cross-section of temperature regimes. Figure B.8 shows the scaling behavior of each proposal method for $T = \{0.1, 1, 10\}$ while Table B.1 shows results of each fit according to Equation 15.

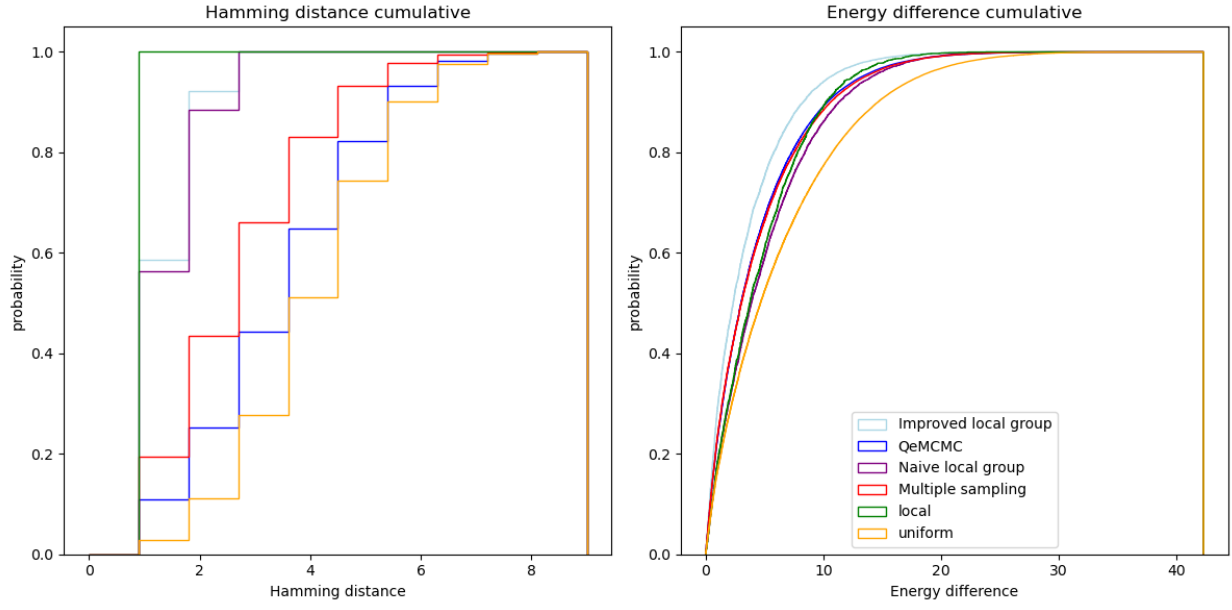


Figure B.6: Cumulative distributions for an example 9 spin problem instance, where the Hamming distance (left) and energy difference (right) of each proposal method are compared. For all CG methods, $q = 3$.

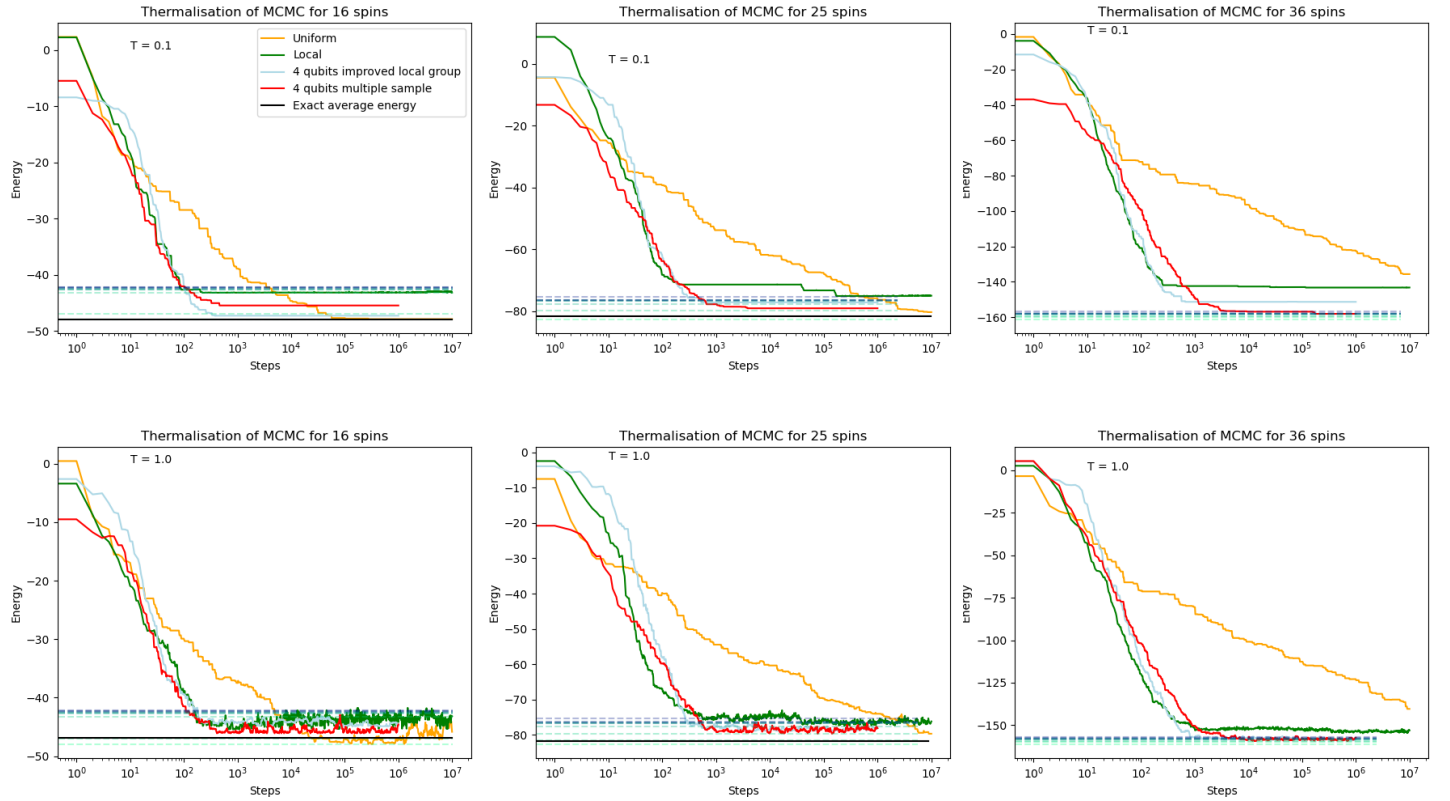


Figure B.7: Average energy thermalisation plot of 10 Markov Chains for one randomly selected Ising model of size 16 (left), 25 (middle) and 36 (right). $T = 0.1$ (top) is clearly a more difficult problem than $T = 1$ (bottom) where the Markov chains acceptance rate is much higher. The coloured dotted lines represent the 10 lowest energy levels of the system, while the black line represents the average Boltzmann energy. This is not provided for the 36 spin system due to the computation limitations of brute force solvers.

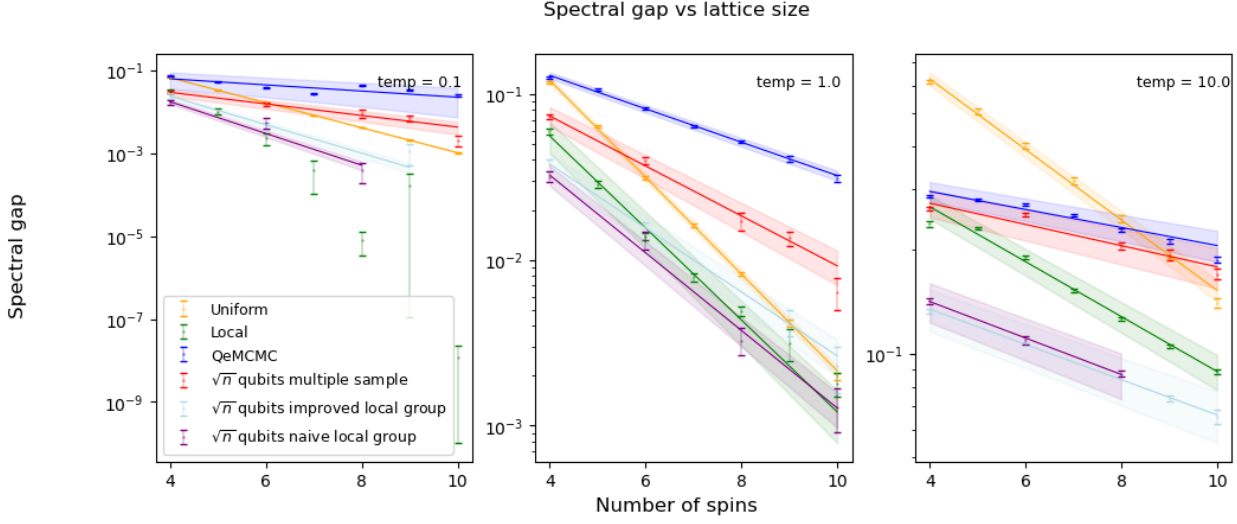


Figure B.8: Scaling of spectral gap with system size for a range of T . Fitting results are given in Table B.8 Classical uniform (orange) and local (green) clearly scale worse than the QeMCMC (blue) as system size increases. Local group (purple) perform variably and the improved local group (light blue) performs better, consistently out-scaling classical methods. Multiple sampling enables (red) CGQeMCMC to almost match QeMCMC in high temperatures, however performance is reduced in low temperatures.

Temperature	0.01	1	10
Uniform	$k = 1.003(2)$	$k = 0.97(1)$	$k = 0.341(8)$
Local	N/A	$k = 0.92(4)$	$k = 0.26(1)$
Quantum	$k = 0.25(8)$	$k = 0.335(8)$	$k = 0.087(1)$
Quantum $q = \sqrt{n}$ local group	$k = 1.27(2)$	$k = 0.77(2)$	$k = 0.177(5)$
Quantum $q = \sqrt{n}$ improved local group	$k = 1.1(2)$	$k = 0.64(2)$	$k = 0.171(5)$
Quantum $q = \sqrt{n}$ multiple sample	$k = 0.46(4)$	$k = 0.50(3)$	$k = 0.10(1)$

Table B.1: Table of results for fits in Figure B.8